Review
Recent Advances in DNA Catalysis

Claudia Höbartner, Scott K. Silverman
Department of Chemistry, University of Illinois at Urbana-Champaign, 600 South Mathews Avenue, Urbana, IL 61801

Received 25 June 2007; revised 17 July 2007; accepted 17 July 2007
Published online 23 July 2007 in Wiley InterScience (www.interscience.wiley.com). DOI 10.1002/bip.20813

ABSTRACT:

Studies of catalytically active DNA sequences have expanded considerably since the first artificial deoxyribozyme was identified in 1994. Nevertheless, the field is still quite young, and advances in both fundamental understanding and practical applications of deoxyribozymes are still developing. Deoxyribozymes that either cleave or ligate two RNA substrates have been most widely investigated, and this review describes recent advances in the fundamental studies and applications of these DNA enzymes. Deoxyribozymes with catalytic activities other than RNA ligation and cleavage are also increasingly pursued, and this review covers several key examples. © *2007 Wiley Periodicals, Inc. Biopolymers 87: 279–292, 2007.*

Keywords: deoxyribozyme; DNA enzyme; DNAzyme; cleavage; ligation

This article was originally published online as an accepted preprint. The "Published Online" date corresponds to the preprint version. You can request a copy of the preprint by emailing the Biopolymers editorial office at biopolymers@wiley.com

INTRODUCTION

Since the identification of the first artificial deoxyribozyme (DNA enzyme, DNAzyme) in 1994,[1] significant progress has been made in our fundamental understanding of DNA's capabilities as a catalyst. Many efforts have also used deoxyribozymes as critical components within analytical applications. This review addresses some of the recent developments in the area of DNA catalysis, with focus on deoxyribozymes that either cleave or ligate two RNA oligonucleotide substrates.

Correspondence to: Scott K. Silverman; e-mail: scott@scs.uiuc.edu
Contract grant sponsors: US National Institutes of Health; David and Lucile Packard Foundation

DEOXYRIBOZYMES THAT CLEAVE RNA

Many RNA-cleaving deoxyribozymes have been reported.[2] The earliest studies provided proof of principle for the basic phenomenon of DNA catalysis,[1,3] and the potential of deoxyribozymes as practical laboratory research tools was quickly recognized.[4] More recent efforts have expanded this potential, and fundamental studies of catalysis and its regulation have been performed. In addition, RNA-cleaving deoxyribozymes are increasingly used as integral components of analytical sensors.

Deoxyribozymes as General and Useful In Vitro Reagents for RNA Cleavage

One of the most widely used deoxyribozymes, the 8–17 deoxyribozyme,[3] is very useful for site-specific cleavage of a wide range of RNA substrates. The name "8–17" pertains to the deoxyribozyme obtained by Santoro and Joyce as the 17th clone from the 8th round of selection; every laboratory has idiosyncratic nomenclature for its deoxyribozymes. RNA cleavage by the 8–17 deoxyribozyme is achieved in high yield and with k_{obs} on the order of 1 min^{-1}, but with the important limitation that only A–G dinucleotide junctions within RNA can be targeted (Figure 1a). To understand the potential scope of DNA-catalyzed RNA cleavage, and also to obtain a collection of practical RNA-cleaving reagents, Li and coworkers sought to generalize deoxyribozymes for cleavage of all possible RNA dinucleotide junctions.[5] Remarkably, a series of parallel in vitro selection experiments converged on a set of deoxyribozymes that each strongly resemble 8–17 in terms of predicted secondary structure (Figure 1b). Collectively, these deoxyribozymes are capable of cleaving 14 of the 16 possible RNA dinucleotide junctions. In addition to its implications regarding basic aspects of nucleic acid

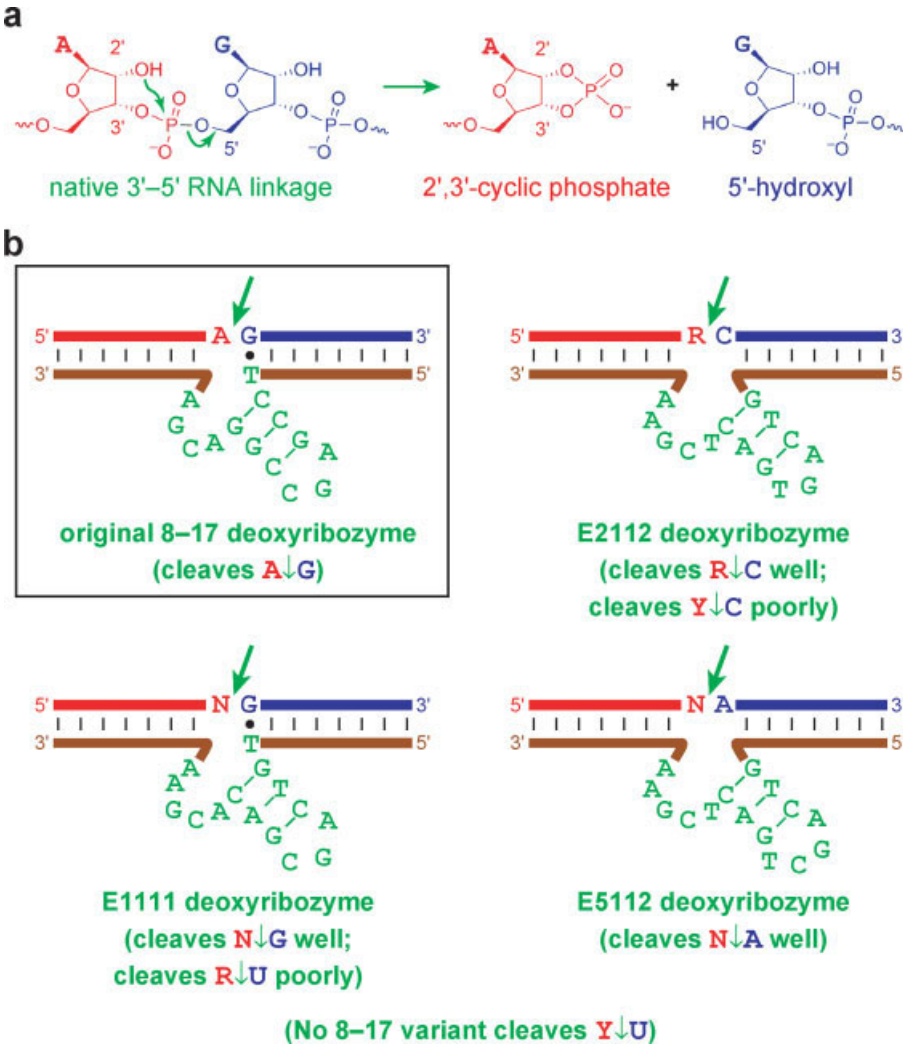

FIGURE 1 The 8–17 deoxyribozyme and its variants, which collectively cleave 14 of the 16 possible RNA ligation junctions.[3,5] (a) The RNA cleavage reaction catalyzed by the 8–17 deoxyribozyme. (b) Detailed depictions of 8–17 and its variants (R, purine; Y, pyrimidine). In the box is the original 8–17 deoxyribozyme, which cleaves only A–G RNA linkages. Three 8–17 variants (E2112, E1111, and E5112 as illustrated) are sufficient to cleave 13 of the remaining 15 linkages. At best, the R–U linkages are cleaved poorly by E1111. No 8–17 variant cleaves Y–U linkages. For preparative RNA cleavage, the original 8–17 deoxyribozyme is typically used with 40–100 m*M* Mg^{2+}, whereas the variants are used in a mixture of Mg^{2+} and 10 m*M* Mn^{2+}.

catalysis,[5,6] this study has provided a well-defined set of deoxyribozymes that allows in vitro cleavage of almost any RNA target sequence. Guidelines for using these 8–17 deoxyribozyme analogs as practical RNA cleavage reagents are provided in Figure 1b.

Structural and Mechanistic Characterization of RNA-Cleaving Deoxyribozymes

A recent effort probed the functional roles of nonbridging phosphate oxygens in the RNA-cleaving 10–23 deoxyribozyme.[7] Nawrot et al. separately replaced each phosphate linkage of 10–23 with a stereorandom phosphorothioate and examined "rescue" of phosphorothioate-suppressed activity by substituting Mn^{2+} for Mg^{2+}. Restoration of phosphorothioate-suppressed activity by Mn^{2+} strongly suggests that the particular phosphate group directly contacts a metal ion. Via this approach, seven particular oxygen atoms within the core of the 10–23 deoxyribozyme were identified as coordinating one or more divalent metal ions. In contrast, in two cases phosphorothioate substitution alone substantially improved the catalytic rate even without adding Mn^{2+}; a

number of explanations for this effect are possible. Further experiments with stereodefined phosphorothioate substitutions revealed differential involvement of pro-R_P and pro-S_P nonbridging oxygen atoms at various phosphate positions. The same study also characterized the role of O^6 of a specific guanosine nucleotide within the 10–23 catalytic core, concluding that this oxygen atom also coordinates a divalent metal ion during catalysis. Particularly in the absence of high-resolution structural information for this or any other deoxyribozyme, such detailed functional analyses will be invaluable for understanding how many DNA enzymes are able to achieve catalysis, regardless of the exact reactions that they catalyze.

An unusual new approach to structural characterization of deoxyribozymes has been reported by Leung and Sen, who examined "electron hole" flow through the folded structure of the 8–17 deoxyribozyme bound to its RNA substrate (which was modified with a 2′-deoxy substitution to prevent catalysis).[8] Photoexcitation of an anthraquinone sensitizer covalently attached at the end of a double-helical region was used to initiate nucleobase radical cation formation. Flow of this "hole" through the double-helical regions of the deoxyribozyme-substrate complex leads to guanine radical cations and subsequently guanine oxidative damage products such as 8-oxoguanine, which may be detected by strand cleavage after treatment with piperidine. Because hole flow depends strongly on the nucleic acid structure, including stacking interactions among the three double-helical secondary structure elements, the hole flow patterns directly report on the structure and folding of the deoxyribozyme. For example, coaxiality among the three helical regions of the deoxyribozyme was probed as a function of Mg^{2+} concentration; the results were similar to those obtained by FRET with a related deoxyribozyme.[9] An active-site cytosine (C23) also showed unusual hole localization, which suggested that this nucleobase is located in an atypical local environment. This environment was assigned by the authors as particularly solvent-accessible, which increases the rate of reaction of water with the nucleobase radical cation. Overall, this new approach of examining electron hole flow patterns through nucleic acid enzymes allows analysis of structural information such as helical stacking preferences that is challenging to obtain by other approaches.

Metal-ion induced global folding of the 8–17 deoxyribozyme and correlations between its structure and activity have recently been studied in great detail by Lu and coworkers using FRET.[10] With either Zn^{2+} or Mg^{2+}, complete folding of the catalytic DNA into a compact structure was observed at lower metal ion concentrations than are needed for saturation of the RNA cleavage activity. Therefore, the deoxyribozyme folds before it catalyzes cleavage, and more metal ion interactions are required to activate catalysis than to initiate folding. In contrast, in the presence of Pb^{2+} (with which the 8–17 deoxyribozyme has highest catalytic activity), no global folding was observed. These results show that the interactions of Pb^{2+} with the DNA are clearly different from those of Zn^{2+} and Mg^{2+}, additionally suggesting that adoption of a compact conformation by a deoxyribozyme may not always be a prerequisite for catalysis.

Photochemical Modulation of DNA-Catalyzed RNA Cleavage

The catalytic activities of RNA-cleaving deoxyribozymes have been modulated by introduction of photocaged nucleotides. Two examples have been reported where DNA catalysis is induced as a consequence of irreversible photodeprotection of covalent nucleobase modifications. First, Perrin and coworkers reported a photoactive C8-modified adenosine building block that was placed into the active site of the Zn^{2+}-dependent 17E deoxyribozyme (Figure 2a).[11] Depending on the exact location of the modified adenosine within the catalytic core, the RNA cleavage activity was either unchanged, strongly perturbed, or completely suppressed. Upon brief irradiation at 280 nm the thioether linkage of the modified adenosine was cleaved, presumably via photoinduced single electron transfer followed by homolysis of the carbon–sulfur bond. This restored an unmodified adenine nucleobase and therefore full deoxyribozyme activity. Second, Deiters and coworkers introduced the 6-nitropiperonyloxymethyl (NPOM) group at the N^3 position of thymidine (Figure 2b), thereby generating a tool for probing the catalytic contributions of specific thymidine hydrogen bonds within the core of the 10–23 deoxyribozyme.[12] Furthermore,

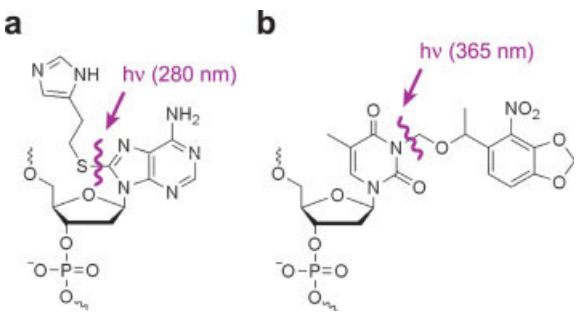

FIGURE 2 Irreversible photochemical modulation of DNA-catalyzed RNA cleavage. In both cases, the photocaged DNA nucleotide is shown; irradiation restores full RNA cleavage activity to the deoxyribozyme in which this nucleotide is incorporated. (a) 8-(2-(4-Imadzolyl)ethyl-1-thio)-2′-deoxyadenosine, which is decaged by irradiation at 280 nm.[11] (b) (6-Nitropiperonyloxymethyl)thymidine, which is decaged by irradiation at 365 nm.[12]

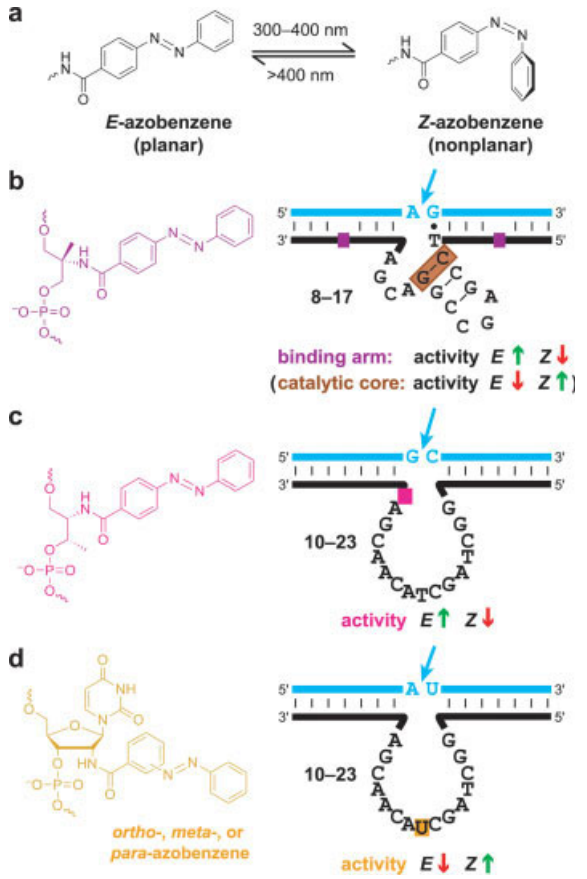

FIGURE 3 Reversible photochemical modulation of DNA-catalyzed RNA cleavage by covalently attached azobenzene. (a) The photostationary state favors the nonplanar *Z* isomer under irradiation with UV light (300–400 nm) or the planar *E* isomer under irradiation with visible light (>400 nm). (b–d) Three examples of reversible photochemical modulation (see text for details).[13–15]

incorporation of several NPOM-derivatized thymidines into the substrate binding arms suppressed RNA cleavage activity by preventing Watson–Crick base-pair interactions between the substrate and the deoxyribozyme. Cleavage of the NPOM moieties upon irradiation with non-photodamaging UV light (365 nm) restored the catalytic activity. These studies with the modified A and T nucleotides are intriguing examples of chemical nucleobase modifications that generate a light-responsive "on switch" for DNA catalytic activity.

Three other studies reported reversible photomodulation of DNA-catalyzed RNA cleavage.[13–15] In all of these cases, the light-induced switching of catalytic activity is based on photochemically induced *E*–*Z* isomerization of one or more covalently attached azobenzene moieties (Figure 3a). Upon irradiation with visible light ($\lambda > 400$ nm), azobenzene exists in the planar *E* configuration that enhances DNA duplex stability by intercalation between base pairs. In contrast, the nonplanar *Z* isomer that is formed by irradiation with UV light (300–400 nm) perturbs optimal base stacking. Using covalently attached azobenzene, Liu and Sen successfully demonstrated reversible photomodulation of the 8–17 deoxyribozyme under single-turnover conditions.[13] Two nucleotides in the substrate binding arms were replaced by azobenzene derivatives that are attached via an amide bond to a 2-amino-2-methylpropanediol linker, which was inserted into the DNA backbone by solid-phase synthesis (Figure 3b). Upon irradiating the modified deoxyribozyme with visible light in the presence of the RNA substrate, a fivefold to sixfold increase in catalytic rate was observed as compared to irradiation with UV light, indicating that the enzyme-substrate complex is stabilized when the azobenzene moieties are in the *E* configuration. A similar result was obtained by Komiyama and coworkers, who incorporated amide-linked *E*-azobenzene via a D-threoninol moiety into the 10–23 deoxyribozyme to enhance cleavage of certain RNA substrates that were difficult to cleave with the parent 10–23 (Figure 3c).[14] The authors showed more generally that incorporation of an intercalating moiety such as anthraquinone, pyrene, or 2-stilbazole at the junction between the catalytic loop and the substrate binding arm leads to higher catalytic activity.

Interestingly, when Liu and Sen appended azobenzene onto the DNA backbone within the catalytic core of the 8–17 deoxyribozyme rather than within the substrate binding arms, RNA cleavage was disfavored rather than favored by the *E*-azobenzene configuration (Figure 3b). The reaction rate was increased after irradiation with UV light, which converted the azobenene into the *Z* configuration.[13] Similarly, rate enhancement by UV irradiation was observed in a separate study in which azobenzene moieties were incorporated into the catalytic core of the 10–23 deoxyribozyme. Keiper and Vyle attached an *ortho*-, *meta*-, or *para*-phenylazobenzoyl group via an amide linkage to the 2′-position of a 2′-amino-2′-deoxyruridine residue at a nonconserved nucleotide in the catalytic loop of 10–23 (Figure 3d). Using this approach, they demonstrated reversible photomodulation under multiple-turnover conditions.[15] Upon irradiation with UV light, up to ninefold enhancement of the RNA cleavage rate was observed, and the catalytic activity reached a level equivalent to that of the unmodified 10–23. Thermal back-isomerization to the *E* isomer (which leads to attenuated RNA cleavage activity) was observed only for the *para*-azobenzene derivative, whereas the *Z* configurations of the *ortho*- and *meta*-photoswitches were stable under the experimental conditions.

These examples demonstrate that the rates of DNA-catalyzed RNA cleavage can be enhanced by presence of either *E* or *Z* azobenzene, depending on the attachment site of the

azobenzene within the deoxyribozyme. While the details are probably idiosyncratic to the individual deoxyribozyme-substrate systems, the general principles will likely transfer to other cases. The development of reversible light-responsive DNA catalysts adds useful regulatory tools to biocatalysis and may expand opportunities for controlling DNA catalytic activity in spatially and temporally well-defined fashion.

Analytical Applications of RNA-Cleaving Deoxyribozymes

Lu and coworkers have reported many deoxyribozyme-based sensors that depend on RNA cleavage as part of the signal transduction process.[16,17] The "readout" in such systems can be based on fluorescent or colorimetric signals; e.g., those involving covalently attached fluorophores or gold nanoparticles. Recently, this group described a highly sensitive detector for uranium when present in the form of the uranyl cation, UO_2^{2+}.[18] In vitro selection was used to identify a deoxyribozyme that cleaves a single ribonucleotide embedded within a DNA substrate strand in the presence of UO_2^{2+} (Figure 4). The substrate strand was labeled with both fluorophore and quencher (at the 5′- and 3′-ends, respectively), and the deoxyribozyme itself also contained a quencher at its 3′-end. This dual-quencher approach had been shown to decrease background signals that arise from incomplete hybridization of the substrate strand to the deoxyribozyme.[19] Using the new deoxyribozyme sensor, the UO_2^{2+} detection limit was 45 p*M* (11 parts per trillion), which is over three orders of magnitude lower than the toxic UO_2^{2+} level in drinking water of 130 n*M* as established by the EPA. This impressive sensitivity was explained by noting the tight (100 n*M*) affinity of UO_2^{2+} for the deoxyribozyme and also

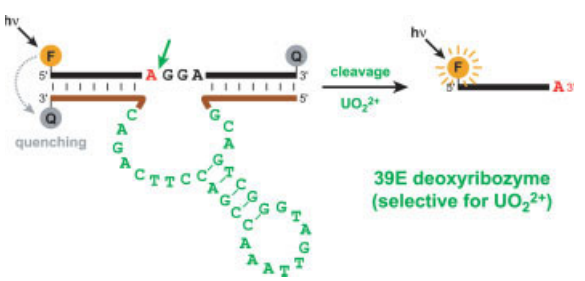

FIGURE 4 The 39E deoxyribozyme that cleaves an RNA linkage only in the presence of uranyl cation (UO_2^{2+}).[18] The substrate strand (black) is all DNA except for a single adenosine ribonucleotide (red). The quencher (Q) on the 3′-end of the deoxyribozyme prevents fluorescence from the fluorescein (F) moiety until UO_2^{2+}-dependent DNA-catalyzed cleavage occurs. The additional quencher on the 3′-end of the substrate strand suppresses fluorescence from any substrate strands that dissociate from the enzyme strand, thereby reducing the background signal.

by considering the multiple-turnover nature of the signal-generation process. The deoxyribozyme was also highly (million-fold) selective for UO_2^{2+} over other metal ions that might typically be present in analytical samples. The detection capability of the deoxyribozyme was validated by comparison to ICP-MS analysis using contaminated soil samples. This report emphasizes that deoxyribozymes have substantial potential for sensor applications in field work.

Expanded practical application of deoxyribozyme-based sensors will likely combine nucleic acid enzymes with common analytical approaches that are not traditionally used with RNA and DNA. As one realization of this goal, Li and coworkers immobilized RNA-cleaving deoxyribozyme sensors for the metal ions Mg^{2+}, Mn^{2+}, Ni^{2+}, and Cd^{2+} within sol–gel matrixes.[20] The deoxyribozymes were equipped with a fluorophore-quencher combination that became separated after metal-catalyzed RNA cleavage when entrapped within either hydrophilic or hydrophobic silica-based sol–gel materials. The precise composition of the sol–gel strongly affected the properties of the deoxyribozyme-based sensors. Although entrapment of the deoxyribozymes lowered both response times and overall signal magnitudes relative to the same deoxyribozymes when free in solution, an advantage of the sol–gel system was the suppression of metal-induced fluorescence quenching. Sol–gel entrapment may also offer protection against nuclease degradation for biologically derived samples or environments. The authors concluded that sol–gel approaches should be useful for deoxyribozyme-based sensors in specific cases, such as multiplexed arrays for diagnostic applications.

Continuing the theme of deoxyribozymes that are not simply free in solution, RNA-cleaving deoxyribozymes were also hybridized with water-soluble multiwalled carbon nanotubes (MWNT).[21] This was achieved by first attaching streptavidin to the nanotube surface (36% coverage) and then binding biotinylated Pb^{2+}-dependent deoxyribozymes to the streptavidin. Over 400 catalytic turnovers were achieved by the nanotube-bound deoxyribozymes, and kinetic comparisons revealed that the presence of the attached MWNT reduced k_{cat} for the deoxyribozyme by only threefold. While this study examined only fundamental aspects of deoxyribozymes interacting with carbon nanotubes, the results suggest that applications which take advantage of the nanomaterial properties of MWNT can also effectively incorporate deoxyribozyme catalysis.

In an alternative immobilized deoxyribozyme assembly, Plaxco and coworkers attached a Pb^{2+}-dependent deoxyribozyme to a gold electrode to create an electrochemical biosensor with parts-per-billion sensitivity.[22] A modified version of the 8–17 deoxyribozyme that bears a methylene blue (MB)

moiety at its 3′-end was hybridized to a DNA substrate containing a single ribonucleotide at the cleavable position. The deoxyribozyme-substrate complex was bound to the gold surface via a 5′-terminal thiol modification on the catalytic DNA strand. Upon Pb^{2+}-dependent cleavage of the scissile phosphodiester bond, the MB moiety transfers electrons to the electrode, leading to a large increase in Faradaic current. This study suggests that immobilization of deoxyribozymes on electrode surfaces offers a promising opportunity for the development of highly sensitive electronic sensors for selective detection of target ions.

RNA-cleaving deoxyribozymes have been applied to detect chemical modifications within RNA.[23] This application is based on the observation that a 2′-*O*-methyl RNA modification at the cleavage site prevents deoxyribozyme-catalyzed RNA cleavage. The method has been used for the qualitative detection of 2′-*O*-ribose methylations in the 18S and 25S rRNAs of *Saccharomyces cerevisiae*. The RNA targets were accessible to cleavage only when isolated from mutant strains lacking specific snoRNAs that are responsible for RNA methylation, thereby suggesting that deoxyribozymes can be used to identify ribose methylations at predicted rRNA sites. Furthermore, the presence of a pseudouridine moiety adjacent to the scissile phosphodiester bond led to a decrease in DNA-catalyzed RNA cleavage efficiency. It was concluded that deoxyribozymes can be used to detect pseudouridine modifications in biologically derived RNAs. Therefore, although quantitation of this approach must be developed further, DNA enzymes may be useful for the verification of bioinformatically predicted RNA modification sites.

DEOXYRIBOZYMES THAT LIGATE RNA

Several years ago, our own group set out to identify deoxyribozymes that ligate RNA. These experiments have been useful both for understanding fundamental aspects of nucleic acid catalysis and for providing practical reagents.

Synthesis of Native 3′–5′ RNA Linkages by Deoxyribozymes

Our initial efforts with RNA ligase deoxyribozymes used two RNA substrates that have 5′-hydroxyl and 2′,3′-cyclic phosphate functional groups (Figure 5a). The regioselectivity in ring-opening of the cyclic phosphate by attack of the 5′-hydroxyl group is very difficult to control, and only non-native 2′–5′ linkages were observed.[24] Subsequent experiments revealed that this preference to form 2′–5′ over native

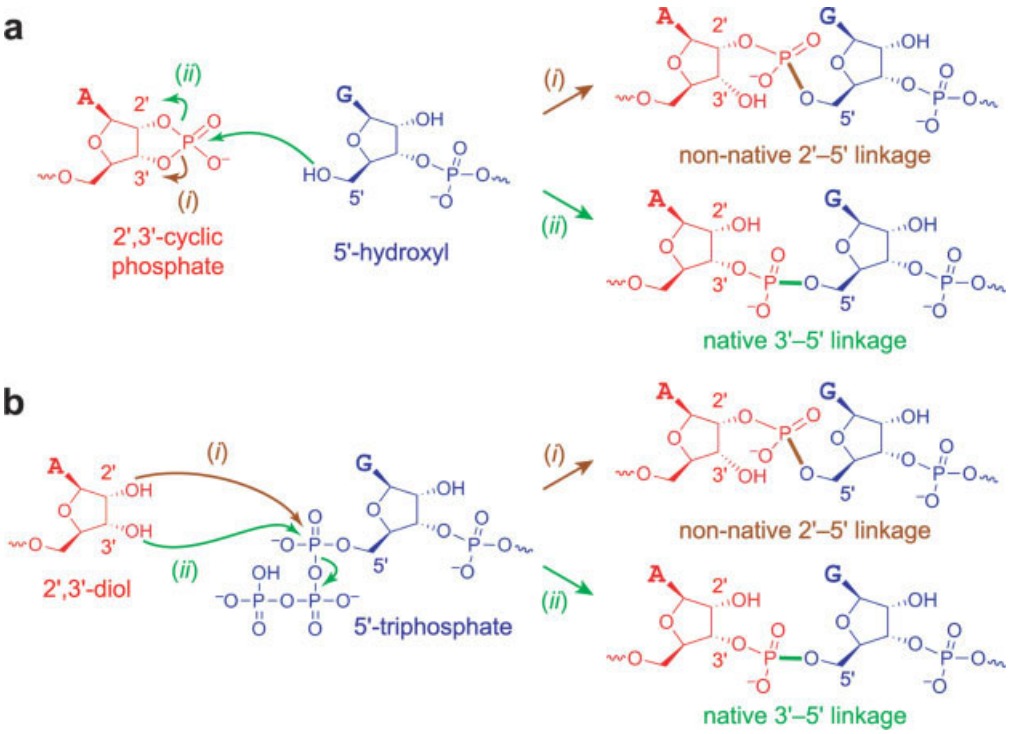

FIGURE 5 RNA ligation to form linear RNA. In both reactions, pathway (*i*) leads to the non-native 2′–5′ linkage, whereas pathway (*ii*) leads to the native 3′–5′ linkage. (a) Ligation using a 2′,3′-cyclic phosphate electrophile. (b) Ligation using a 5′-triphosphate electrophile.

3′–5′ linkages is maintained in a variety of structural contexts, although the chemical reason underlying this preference is not known.[25] The DNA-catalyzed synthesis of 3′–5′ linkages using this particular RNA substrate combination is an ongoing challenge.

We have also used RNA substrates that have 2′,3′-diol and 5′-triphosphate functional groups (Figure 5b), with much more success in forcing the newly formed linkage to be 3′–5′. In one selection experiment we embedded the RNA ligation site in the context of a Watson–Crick duplex, which enforced highly site-selective formation of 3′–5′ linkages because these junctions are more stable than 2′–5′ linkages in an RNA-DNA duplex.[26] Unfortunately, the resulting deoxyribozymes were insufficiently tolerant of different RNA sequences to be generally useful. In another selection experiment, the same strategy that was used for the cyclic phosphate substrate combination was employed, with a key addition. By incorporating an additional selection step using an RNA-cleaving deoxyribozyme that is highly selective for cleaving 3′–5′ linkages, we ensured that nearly all newly created bonds between the two RNA substrates were formed by nucleophilic attack of the 3′-hydroxyl group (and not the 2′-hydroxyl group) at the 5′-triphosphate.[27] Using this modified selection strategy, we identified both Mg^{2+}- and Zn^{2+}-dependent deoxyribozymes that form native 3′–5′ linkages and also have useful ligation rates (0.01–0.06 min^{-1}, corresponding to $t_{1/2}$ on the order of 10 min to 1 h), yields, and RNA substrate sequence generality.[28] Our current efforts seek to establish a set of RNA ligase deoxyribozymes that collectively allow 3′–5′ ligation of any two RNA substrates regardless of sequence, similar to the collection of RNA-cleaving deoxyribozymes illustrated in Figure 1.

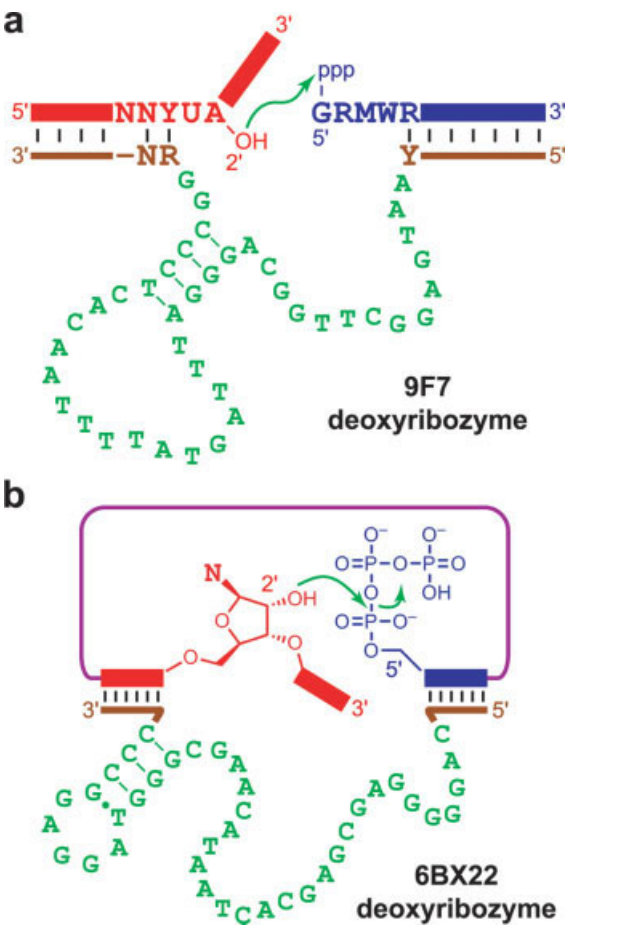

FIGURE 6 RNA ligation to form branched and lariat RNA. (a) Formation of 2′,5′-branched RNA by reaction of an internal 2′-OH group with a 5′-triphosphate. Depicted is the 9F7 deoxyribozyme, which has many RNA sequence requirements near the ligation site.[29,30] N, any nucleotide; M, A or C; W, A or U. (b) Formation of lariat RNA when the two reacting functional groups are within the same RNA molecule. Depicted is the 6BX22 deoxyribozyme, which has considerable generality for creating lariat RNA.[31]

Synthesis of 2′,5′-Branched and Lariat RNA by Deoxyribozymes

In our initial deoxyribozyme selection experiments with the 2′,3′-diol and 5′-triphosphate RNA substrate combination, the ligated RNA products were 2′,5′-branched rather than linear.[29] The selection strategy permitted formation of these branched products because the only requirement for successful catalysis was that the DNA should join the two RNA substrates, and an internal RNA 2′-hydroxyl group (rather than the terminal 2′- or 3′-hydroxyl group) could readily serve as a nucleophile to react with the 5′-triphosphate (Figure 6a). The new deoxyribozymes had rather specific sequence requirements for the RNA substrates near the ligation junction, which suggests interesting three-dimensional structure at the active site.[30] These sequence requirements also precluded general use of the new deoxyribozymes for branched RNA synthesis. Interestingly, the new deoxyribozymes could also form lariat rather than simply 2′,5′-branched RNA (Figure 6b), and we subsequently identified a different deoxyribozyme that is more general for lariat RNA formation.[31] The latter deoxyribozyme could be used for synthesis of biologically related lariat RNAs that have hundreds of nucleotides in the loop, demonstrating a remarkable site-selectivity by activating only one 2′-hydroxyl group as the nucleophile in the branch-forming reaction.

In a subsequent selection effort we identified the very interesting 7S11 deoxyribozyme, which also forms branched RNA by joining an internal 2′-hydroxyl group and a 5′-triphosphate.[32] Although the selection strategy that led to 7S11 originally positioned the random DNA region between two Watson–Crick "binding arms" in the conventional way, the

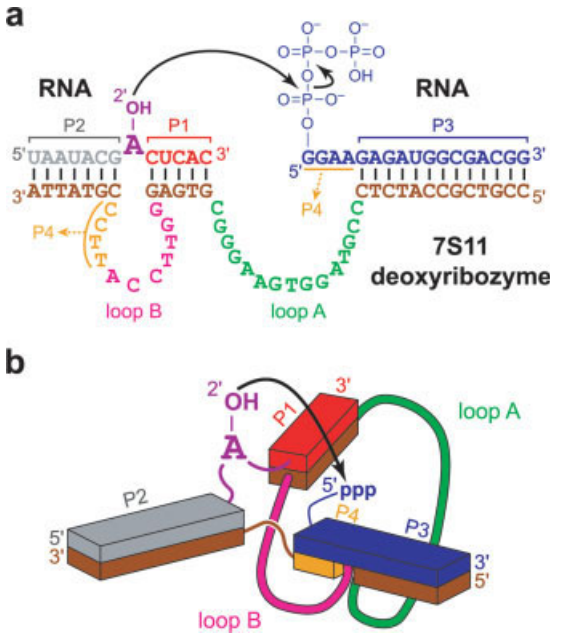

FIGURE 7 The 7S11 deoxyribozyme, which forms 2′,5′-branched RNA via a three-helix-junction (3HJ) complex among itself and its two RNA substrates.[32–34] (a) Secondary structure, depicting the four paired regions (P1–P4). (b) Approximate three-dimensional model emphasizing the 3HJ structure. Not depicted is the finding that an oligonucleotide can serve as leaving group in place of pyrophosphate.

final deoxyribozyme replaced one of the binding arms with part of the random region itself, thereby locating the branch-site nucleophile between two Watson–Crick RNA-DNA helices (Figure 7a). The deoxyribozyme-RNA complex adopts a three-helix-junction (3HJ) architecture in which all of the base-paired regions have extensive Watson–Crick complementarity (Figure 7b).[33] Many changes to the RNA nucleotides are tolerated with high ligation activity as long as the corresponding DNA nucleotides are changed to maintain the complementarity. Therefore, the 7S11 deoxyribozyme has broad generality for synthesizing branched RNA with only modest sequence restrictions. As described later, 7S11 has formed the basis for a wide range of subsequent experiments in our laboratory.[34–37]

One particular selection experiment after the discovery of 7S11 was used to provide information on the conserved role of the "branch-site adenosine" nucleotide in pre-mRNA splicing.[35] Nature almost always uses adenosine as the branch-site nucleotide during the first step of RNA splicing, in which the 5′-splice site is cleaved by attack of the branch-site 2′-hydroxyl group. In the selection experiment that led to 7S11 itself (see earlier), the branch-site nucleotide was adenosine. Although this was intriguing, ultimately the data did not compel any chemical conclusion about the origin of branch-site adenosine conservation in nature. To explore this further, we selected new deoxyribozymes in the 3HJ format typified by 7S11, but we provided a branch-site uridine rather than adenosine during the selection process. Despite never having the opportunity to use adenosine during the selection itself, the resulting deoxyribozymes still had a substantial preference for branch-site adenosine. This indicates that adenosine is inherently favored as the branch-site nucleophile, at least in the structural context maintained by 7S11 and its variants. The atomic-level explanation for this adenosine preference requires a detailed biochemical investigation.

Applications of Deoxyribozymes that Ligate RNA

A side benefit of the "branch-site adenosine" investigation was the identification of a 7S11 variant, 10DM24, that is even more sequence-tolerant than 7S11 itself. Using 10DM24, we developed a new approach for site-specific DEoxyribozyme-CAtalyzed Labeling of RNA that we named DECAL (Figure 8).[36] In the DECAL approach, the two substrates for branch formation are viewed as a large target RNA and a smaller tagging RNA modified with a biophysical label. Branch formation catalyzed by 10DM24 attaches the tagging RNA to the desired 2′-hydroxyl group of the target RNA. The tagging RNA is a transcript with a single 5-aminoallylcytidine nucleotide at its second position, with the aminoallyl group post-transcriptionally modified with an amine-reactive probe such as fluorescein NHS ester. Using DECAL, we showed that the P4–P6 domain of the *Tetrahymena* group I intron RNA could be derivatized with both fluorescein and tetramethylrhodamine (TAMRA) tags that enable subsequent FRET analysis. We anticipate that the DECAL strategy will be particularly useful for labeling of very large target RNAs such as group II introns and ribosomal RNAs, which are extremely challenging to prepare in site-specifically modified form by other approaches such as splint ligation.

Several efforts have used deoxyribozymes to prepare branched RNAs that facilitated biochemical studies. Using the 7S11 deoxyribozyme, branched RNAs related to the group II intron splicing intermediate were synthesized. These branched RNAs allowed an explicit test of a decade-old hypothesis concerning the reversibility of the first step of RNA splicing.[37] Separately, the 6CE8 deoxyribozyme was identified that synthesizes 2′,5′-branched RNA with any branch-site nucleotide.[38] This deoxyribozyme was applied to prepare the branched RNA that had been proposed as an intermediate in Ty1 retrotransposition; despite its importance to a biochemical hypothesis, this branched RNA had not been independently prepared. Using the proposed Ty1 branched RNA, we showed that Ty1 reverse transcriptase cannot read

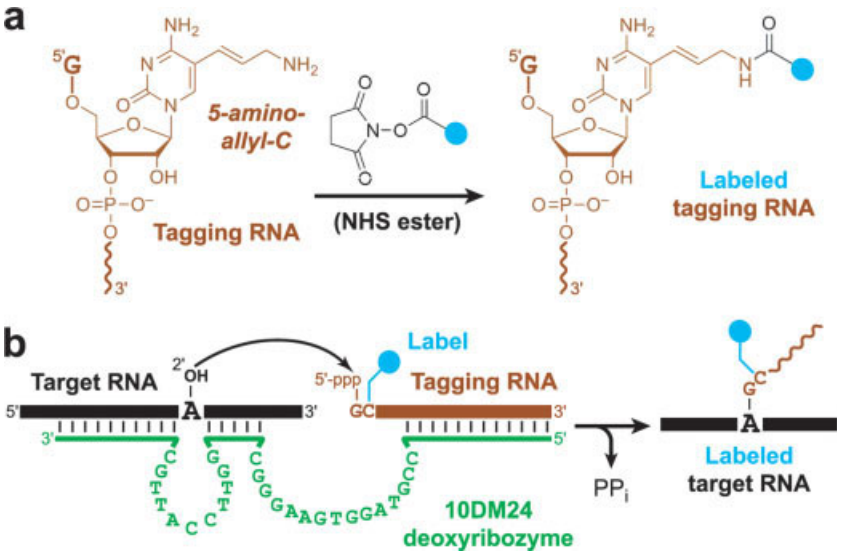

FIGURE 8 Deoxyribozyme-catalyzed labeling (DECAL) of RNA.[36] (a) Generation of the labeled tagging RNA by reaction of an aminoallyl-modified nucleotide with the *N*-hydroxysuccinimide (NHS) ester of a biophysical label (e.g., fluorescein; biotin). (b) Attachment of the tagging RNA to the target RNA by the 10DM24 deoxyribozyme.

through the branch site with high enough efficiency to explain the presence of Ty1 cDNA in cells that lack debranching enzyme, which would hydrolyze the proposed branch before reverse transcription.[39] Therefore, the 6CE8 deoxyribozyme allowed an explicit test of a biochemical hypothesis in a fashion that was essentially unachievable by other methods.

Conversion of a RNA Ligase Ribozyme into a Deoxyribozyme by In Vitro Evolution

Functional nucleic acids made out of RNA generally lack function when the same sequence is prepared as DNA, and vice versa. Exceptions are known for a riboflavin RNA aptamer that retains partial binding activity when made as DNA[40] and for a hemin-dependent peroxidase deoxyribozyme that has full catalytic activity when made as RNA.[41] To explore the relationship between RNA and DNA catalysis, Joyce and coworkers used in vitro selection to convert a known RNA ligase ribozyme into a deoxyribozyme.[42] Although the parent ribozyme was inactive when made as DNA, the selection process was able to identify a variant DNA sequence with good activity. The new deoxyribozyme sequence is not active when made as RNA. A remaining challenge is therefore to find ligase sequences that are active as both RNA and DNA. More generally, identifying single nucleotide sequences that are functional as either RNA or DNA should offer insight into fundamental aspects of "crossover" between two informational systems that are based on closely related—but clearly distinct—biopolymers.

DEOXYRIBOZYMES WITH OTHER CATALYTIC ACTIVITIES

Beyond RNA cleavage and ligation lies a vast number of bioorganic reactions that could potentially be catalyzed by DNA. Only a tiny fraction of such reactions have been investigated, and to date all of these involve nucleic acids as substrates. The highest rate enhancement yet reported for a DNA enzyme, 10^{10}, was found for a deoxyribozyme that adenylates (caps) its own 5′-terminus.[43]

Recurrence of a Self-Phosphorylating Deoxyribozyme Motif

Li and coworkers have identified numerous self-phosphorylating deoxyribozymes that use GTP as the phosphate donor.[44–46] Although the experimental data establish that several of the deoxyribozymes arose independently during selection, a conserved catalytic core was identified that is common to all of the deoxyribozymes. As the authors noted,[46] such independent in vitro isolation of a recurrent motif has been observed for both the natural hammerhead ribozyme[47] and for the artificial 8–17 deoxyribozyme.[5] In all of these cases, including the self-phosphorylating deoxyri-

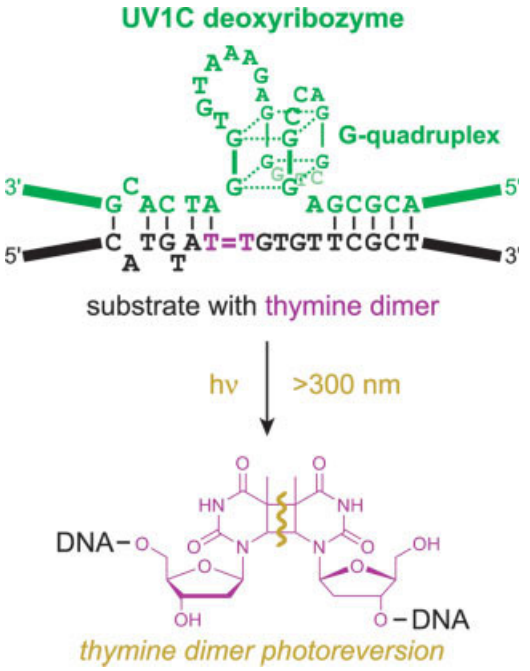

FIGURE 9 The UV1C deoxyribozyme, which catalyzes thymine dimer photoreversion.[48,49] The G-quadruplex acts as an "antenna" to absorb light of wavelengths not normally absorbed by nucleic acids.

bozymes, a reasonable conclusion is that the identified motif is the simplest structural solution for the given catalytic activity.

Studies of a Photolyase Deoxyribozyme

Chinnapen and Sen reported a deoxyribozyme, UV1C, with the unusual ability to photocleave thymine cyclobutane dimers (Figure 9).[48] In their original selection design, serotonin was intended to be the UV-absorbing species, but the resulting deoxyribozymes adopted a G-quadruplex structure that allows serotonin-independent absorption of relatively long-wavelength (>300 nm) light. Subsequent mechanistic studies provided additional information about the relative spatial orientation of the G-quadruplex and the thymine dimer moiety within the deoxyribozyme-substrate complex.[49] This set of studies is particularly interesting because it shows that DNA can directly use light energy as part of a catalytic process. The authors' original goal of cofactor-dependent photochemistry—where the cofactor, not the DNA, absorbs the light—remains to be achieved.

Recent Applications of a Peroxidase Deoxyribozyme

A deoxyribozyme with peroxidase activity was applied for the development of new DNA detection methods that are alternatives to DNA quantification by real-time-PCR.[50–52] These new methods use either a colorimetric readout based on the ability of the peroxidase deoxyribozyme to produce a green product by oxidation of 2,2′-azino-bis(3-ethly-benzthiazoline)-6-sulfonate ($ABTS^{2-}$) with H_2O_2 as cosubstrate[53] or a chemiluminescent readout based on the emission of light generated from luminol and H_2O_2 (Figure 10a).[54]

In a PCR-based method, deoxyribozyme-containing primers were used for amplification of the target DNA (Figure 10b).[50] The catalytic DNA sequence was sequestered in the 5′-portion of the PCR primers by Watson–Crick base-pairing within a stem-loop structure. The hairpin-primers also contained a non-extendable hexaethylene glycol unit in the loop region and a single-stranded 3′-extension that is complementary to the target DNA. Amplification of the analyte DNA results in unzipping of the hairpin structure and liberation of the single-stranded deoxyribozyme. This deoxyribozyme then folds into a G-quadruplex structure that binds hemin to form the active peroxidase complex. This leads to formation of either multiple copies of the colored $ABTS^{\bullet-}$ product or chemiluminescence from luminol and H_2O_2, providing a colorimetric or chemiluminescent signal. The hexaethylene glycol linker prevents polymerase extension and assures that the deoxyribozyme portion remains single-stranded. Proof of principle for ultrasensitive DNA detection was obtained by quantification of phage M13 ssDNA with an experimental detection limit of 1.2×10^{-18} *M* (1.2 a*M*), which amounts to ~40 analyte molecules in a 50 μL sample.

In an alternative approach reported independently by Willner and coworkers[51] and Mao and coworkers,[52] the detection of target DNA was based on isothermal DNA amplification (Figure 10c). In polymerase-mediated rolling-circle amplification (RCA), multiple copies of the peroxidase deoxyribozyme are generated in a linear array. The RCA template is a single-stranded circular DNA that contains a recognition sequence complementary to the target DNA as well as one or several units of the complementary deoxyribozyme sequence. The analyte DNA can hybridize to the circular DNA template and serve as the primer for isothermal DNA synthesis mediated by DNA polymerase. Upon binding of hemin, the complex is activated and leads to either a colorimetric or chemiluminescent signal. An RCA protocol was used for the analysis of phage M13 ssDNA with a detection limit of 1×10^{-14} *M* (10 f*M*).[51] The considerably higher sensitivity of the PCR (non-isothermal) amplification method mentioned earlier is attributed to exponential amplification during PCR compared to linear amplification during RCA. Nevertheless, the isothermal RCA process can be experimentally advantageous in terms of speed and operational convenience.

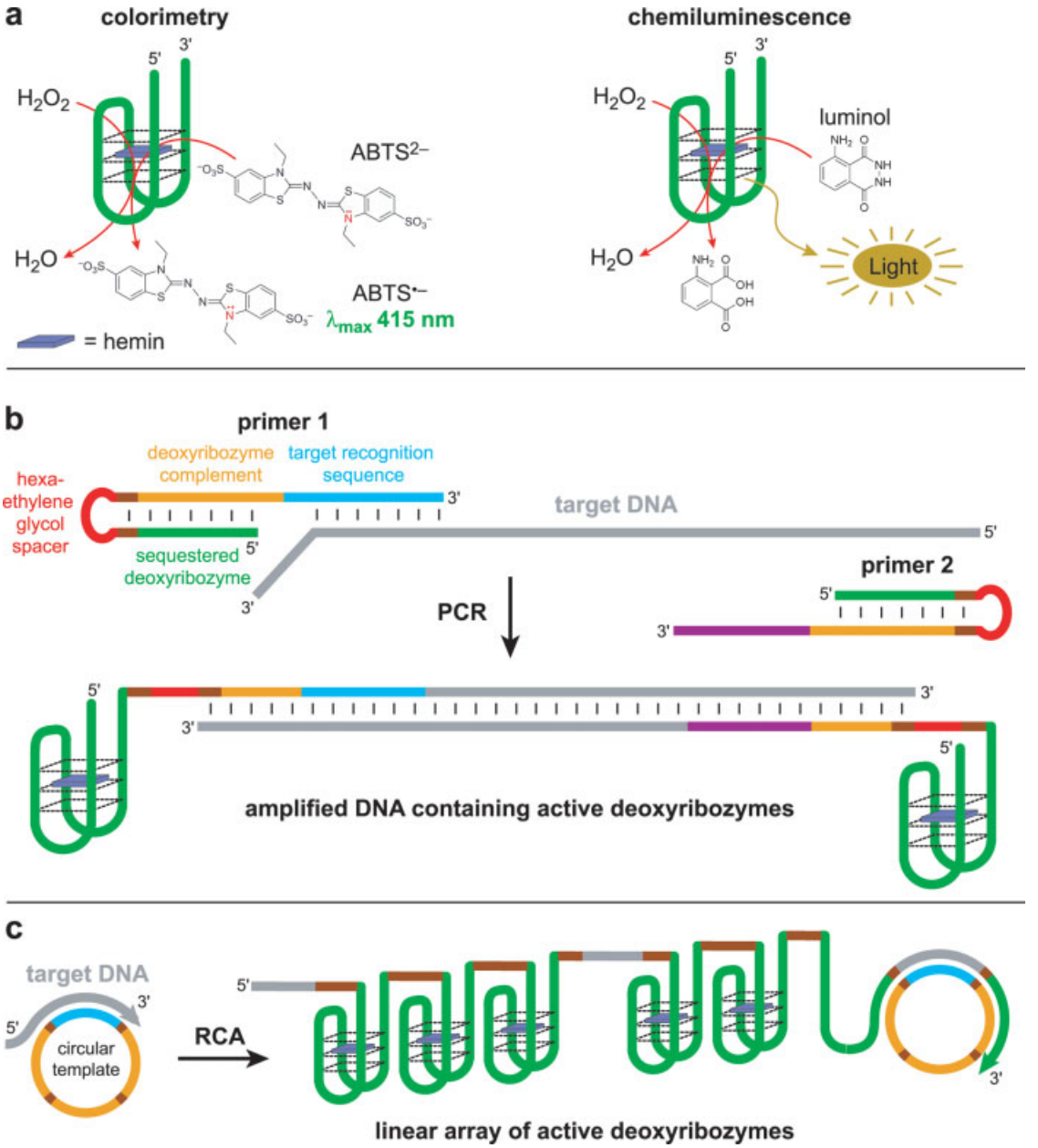

FIGURE 10 DNA detection based on a peroxidase deoxyribozyme. (a) The active peroxidase deoxyribozyme folds into a G-quadruplex structure in the presence of hemin. This complex generates a colorimetric readout by H_2O_2-dependent oxidation of ABTS^{2-} to the green ABTS$^{\bullet-}$,[53] or it generates a chemiluminescent readout from luminol and H_2O_2.[54] (b) PCR-based detection of target DNA using deoxyribozyme-containing hairpin primers.[50] The process uses specially designed hairpin primers that contain the peroxidase deoxyribozyme sequence (green) sequestered in a stem-loop structure; a non-extendable hexaethylene glycol linker in the loop (red); and a single-stranded 3′-extension (blue in primer 1, purple in primer 2) that serves for target recognition. Polymerase extension stops at the hexaethylene glycol moiety, which leads to liberation of the single-stranded deoxyribozyme strand that folds into the active peroxidase in the presence of hemin. (c) DNA detection based on rolling-circle amplification (RCA).[51,52] The circular template contains a target recognition sequence (blue) and several units of the complement of the deoxyribozyme sequence (orange), separated by short DNA spacers (brown). The target DNA serves as primer for isothermal polymerase-mediated synthesis of a linear array of peroxidase deoxyribozymes that fold into the active G-quadruplex structures in the presence of hemin.

Finally, in a separate strategy also by Willner and coworkers, the peroxidase deoxyribozyme has been used for the detection of small molecule analytes and proteins by engineered aptamer-deoxyribozyme composites.[55] The "aptasensor" consist of two DNA strands. One oligonucleotide contains an analyte-specific aptamer and the peroxidase deoxyribozyme; a separate blocking oligonucleotide is partially complementary to both the aptamer and the deoxyribozyme. Hybridization of the blocking oligonucleotide and the aptamer-deoxyribozyme conjugate prevents formation of the active DNA catalyst. In the presence of the analyte (ligand), formation of the aptamer-ligand complex leads to dissociation of the blocking oligonucleotide and subsequent correct folding of the deoxyribozyme into the active G-quadruplex conformation. The detection of the ligand (i.e., the binding event of analyte to the DNA aptamer) is amplified by the DNA-catalyzed oxidation of $ABTS^{2-}$ in the presence of hemin and H_2O_2 to generate a colorimetric readout. Proof of principle was obtained for the analysis of AMP with a detection limit of 4×10^{-6} *M* (4 μM) and lysozyme with a detection limit of 1×10^{-13} *M* (0.1 p*M*). In both cases, this new concept for generating a biocatalytic readout by using blocked deoxyribozyme-aptamer composites allows for comparable or improved detection limits as compared to previously reported colorimetric and electrochemical sensors based solely on aptamers.[56,57]

DNA-Catalyzed Periodate-Dependent Depurination

Our own laboratory recently attempted to select for a deoxyribozyme that uses UDP-GlcNAc as a small-molecule donor of the sugar moiety GlcNAc.[58] The original design was intended to identify deoxyribozymes that attach GlcNAc to either the DNA 5′-hydroxyl group or to the hydroxyl group of a serine residue attached as part of a tripeptide at the 5′-terminus of the DNA. Because the attachment of GlcNAc to the DNA would result in only a minimal PAGE shift, subsequent $NaIO_4$ oxidation of the vicinal diol at positions 3 and 4 of the GlcNAc was expected to provide aldehyde functional groups that could be joined to a 3′-NH_2 oligonucleotide by reductive amination. The extra mass of the 3′-NH_2 oligonucleotide would lead to a PAGE shift, allowing separation of the catalytically active deoxyribozymes. Surprisingly, the selection experiments led to a deoxyribozyme that survived the selection procedure not by attaching GlcNAc but by undergoing highly site-selective $NaIO_4$-dependent (and UDP-GlcNAc-independent) depurination of its 5′-terminal guanosine nucleotide (Figure 11). This outcome highlights the challenges inherent in preventing unforseen ways that DNA sequences can survive the selection procedure by catalyzing a reaction other than the desired transformation. This outcome also underscores the difficulty in learning how to use DNA for reactions that involve small molecule substrates such as UDP-GlcNAc.

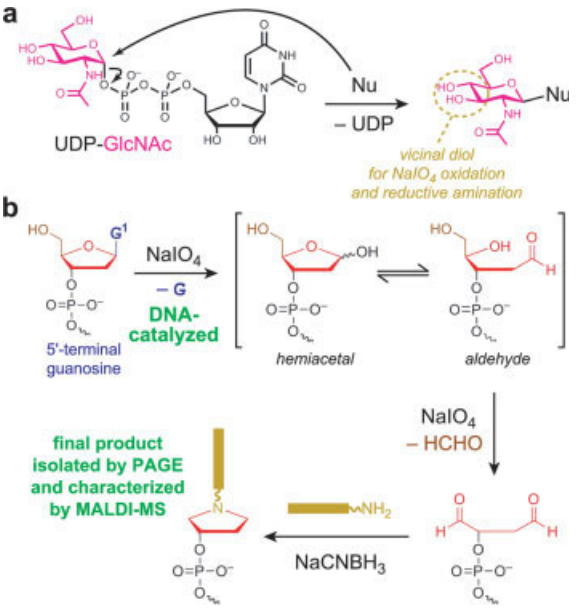

FIGURE 11 Site-selective periodate-dependent depurination of DNA by a deoxyribozyme.[58] (a) Intended reaction of UDP-GlcNAc as an electrophile. The nucleophile (Nu) was intended to be either a DNA 5′-OH group or a side chain of a serine residue attached to the DNA as part of a tripeptide. The vicinal diol of the GlcNAc (circled) was intended for subsequent oxidation by $NaIO_4$ and reductive amination, which would lead to a PAGE shift of the DNA. (b) The deoxyribozyme that emerged from the selection process catalyzes a UDP-GlcNAc-independent but $NaIO_4$-dependent oxidation of the 5′-terminal guanosine of the DNA. To isolate the product and demonstrate its structure, the aldehyde moiety revealed by the depurination was reductively aminated with a 3′-NH_2-oligonucleotide and $NaCNBH_3$.

Building a Selective Small-Molecule Binding Site into a Deoxyribozyme

To understand how to build a small-molecule binding site into a deoxyribozyme, we subsequently re-examined the 10DM24 branch-forming deoxyribozyme. Its 3HJ architecture led us to speculate that disconnecting the guanosine nucleotide that provides the reactive 5′-triphosphate group from the remainder of the oligonucleotide substrate would allow 10DM24 to use GTP as a small-molecule substrate (Figure 12a). We were pleased to find that this strategy works well; GTP is used as a substrate in high yield and in multiple-turnover fashion.[59] Moreover, ATP in place of GTP is accepted as a substrate only when the corresponding deoxyribozyme nucleotide is swapped from C to T, indicating that

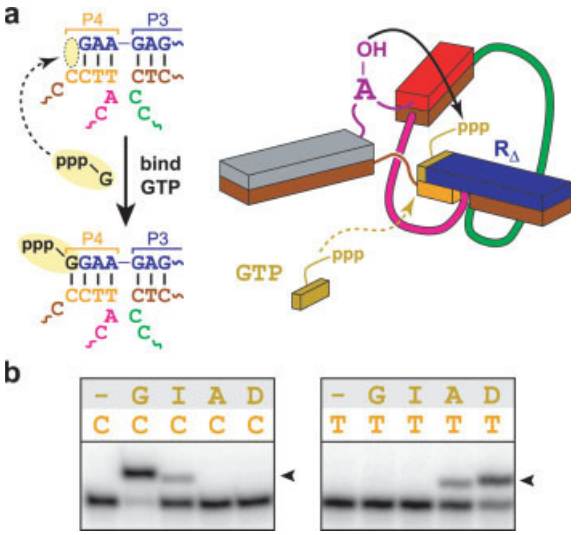

FIGURE 12 Engineering the 10DM24 deoxyribozyme to use an NTP as a small-molecule substrate.[59] (a) Design of the system. Removing the 5′-terminal nucleotide from the right-hand RNA substrate of Figure 7 leaves a binding site for GTP, which pairs with C in the deoxyribozyme. (b) PAGE data showing Watson–Crick covariation for NTP binding and also that the catalytic activity correlates with the number of Watson–Crick hydrogen bonds between the deoxyribozyme and NTP (I, inosine; D, 2,6-diaminopurine ribonucleoside). The arrowhead denotes the ligation product.

the NTP substrate is held in the substrate binding site by Watson–Crick hydrogen bonds (Figure 12b). Consistent with this conclusion, inosine triphosophate (ITP) has a lower reaction rate than GTP whereas 2,6-diaminopurine ribonucleoside triphosphate (DTP) has a higher reaction rate than ATP (i.e., increasing the number of hydrogen bonds improves the rate of catalysis). By testing a small series of GTP analogs, we also showed that preorganization within the substrate is critical to efficient ligation. Overall, this success with engineering a selective small-molecule binding site into the 10DM24 deoxyribozyme indicates that a rational approach is feasible for the use of small-molecule substrates by DNA catalysts.

PERSPECTIVE ON DNA CATALYSIS

Further advances in DNA catalysis will almost certainly require the exploration of a wide variety of bioorganic reactions beyond RNA cleavage and ligation. For instance, no deoxyribozyme has yet been reported that can catalyze any C–C bond-forming reaction, although ribozymes with such activities are known.[60–62] A key challenge for DNA catalysis is to develop deoxyribozymes that can use small molecules, proteins, and other desirable targets as substrates. We also must learn more about deoxyribozyme mechanisms, and this will require high-resolution structural information as obtained by X-ray crystallography or NMR spectroscopy. To date, no catalytically relevant deoxyribozyme structures have been determined by any approach,[63] so this is clearly a fruitful area for new research. In conclusion, the understanding of deoxyribozymes as established by the past dozen or so years of research provides a strong foundation for the ongoing efforts in many laboratories to expand the boundaries of DNA catalysis and to apply deoxyribozymes in a range of practical applications.

C.H. was the recipient of an Erwin Schrödinger Fellowship from the Austrian Science Fund. S.K.S. is a Fellow of the David and Lucile Packard Foundation. Research on deoxyribozymes in the Silverman laboratory has been supported by the NIH, Burroughs Wellcome Fund, March of Dimes, ACS-PRF, and NSF.

REFERENCES

1. Breaker, R. R.; Joyce, G. F. Chem Biol 1994, 1, 223–229.
2. Silverman, S. K. Nucleic Acids Res 2005, 33, 6151–6163.
3. Santoro, S. W.; Joyce, G. F. Proc Natl Acad Sci USA 1997, 94, 4262–4266.
4. Pyle, A. M.; Chu, V. T.; Jankowsky, E.; Boudvillain, M. Methods Enzymol 2000, 317, 140–146.
5. Cruz, R. P. G.; Withers, J. B.; Li, Y. Chem Biol 2004, 11, 57–67.
6. Silverman, S. K. Chem Biol 2004, 11, 7–8.
7. Nawrot, B.; Widera, K.; Wojcik, M.; Rebowska, B.; Nowak, G.; Stec, W. J. FEBS J 2007, 274, 1062–1072.
8. Leung, E. K.; Sen, D. Chem Biol 2007, 14, 41–51.
9. Liu, J.; Lu, Y. J Am Chem Soc 2002, 124, 15208–15216.
10. Kim, H. K.; Liu, J.; Li, J.; Nagraj, N.; Li, M.; Pavot, C. M.; Lu, Y. J Am Chem Soc 2007, 129, 6896–6902.
11. Ting, R.; Lermer, L.; Perrin, D. M. J Am Chem Soc 2004, 126, 12720–12721.
12. Lusic, H.; Young, D. D.; Lively, M. O.; Deiters, A. Org Lett 2007, 9, 1903–1906.
13. Liu, Y.; Sen, D. J Mol Biol 2004, 341, 887–892.
14. Asanuma, H.; Hayashi, H.; Zhao, J.; Liang, X.; Yamazawa, A.; Kuramochi, T.; Matsunaga, D.; Aiba, Y.; Kashida, H.; Komiyama, M. Chem Commun 2006, 5062–5064.
15. Keiper, S.; Vyle, J. S. Angew Chem Int Ed 2006, 45, 3306–3309.
16. Li, J.; Zheng, W.; Kwon, A. H.; Lu, Y. J Am Chem Soc 2000, 122, 10466–10467.
17. Lu, Y. Chem Eur J 2002, 8, 4589–4596.
18. Liu, J.; Brown, A. K.; Meng, X.; Cropek, D. M.; Istok, J. D.; Watson, D. B.; Lu, Y. Proc Natl Acad Sci USA 2007, 104, 2056–2061.
19. Liu, J.; Lu, Y. Anal Chem 2003, 75, 6666–6672.
20. Shen, Y.; Mackey, G.; Rupcich, N.; Gloster, D.; Chiuman, W.; Li, Y.; Brennan, J. D. Anal Chem 2007, 79, 3494–3503.
21. Yim, T. J.; Liu, J.; Lu, Y.; Kane, R. S.; Dordick, J. S. J Am Chem Soc 2005, 127, 12200–12201.
22. Xiao, Y.; Rowe, A. A.; Plaxco, K. W. J Am Chem Soc 2007, 129, 262–263.
23. Buchhaupt, M.; Peifer, C.; Entian, K. D. Anal Biochem 2007, 361, 102–108.
24. Flynn-Charlebois, A.; Wang, Y.; Prior, T. K.; Rashid, I.; Hoadley, K. A.; Coppins, R. L.; Wolf, A. C.; Silverman, S. K. J Am Chem Soc 2003, 125, 2444–2454.
25. Semlow, D. R.; Silverman, S. K. J Mol Evol 2005, 61, 207–215.

26. Coppins, R. L.; Silverman, S. K. J Am Chem Soc 2004, 126, 16426–16432.
27. Wang, Y.; Silverman, S. K. Biochemistry 2005, 44, 3017–3023.
28. Purtha, W. E.; Coppins, R. L.; Smalley, M. K.; Silverman, S. K. J Am Chem Soc 2005, 127, 13124–13125.
29. Wang, Y.; Silverman, S. K. J Am Chem Soc 2003, 125, 6880–6881.
30. Wang, Y.; Silverman, S. K. Biochemistry 2003, 42, 15252–15263.
31. Wang, Y.; Silverman, S. K. Angew Chem Int Ed 2005, 44, 5863–5866.
32. Coppins, R. L.; Silverman, S. K. Nat Struct Mol Biol 2004, 11, 270–274.
33. Coppins, R. L.; Silverman, S. K. J Am Chem Soc 2005, 127, 2900–2907.
34. Coppins, R. L.; Silverman, S. K. Biochemistry 2005, 44, 13439–13446.
35. Zelin, E.; Wang, Y.; Silverman, S. K. Biochemistry 2006, 45, 2767–2771.
36. Baum, D. A.; Silverman, S. K. Angew Chem Int Ed 2007, 46, 3502–3504.
37. Wang, Y.; Silverman, S. K. ACS Chem Biol 2006, 1, 316–324.
38. Pratico, E. D.; Wang, Y.; Silverman, S. K. Nucleic Acids Res 2005, 33, 3503–3512.
39. Pratico, E. D.; Silverman, S. K. RNA 2007, 13, in press. DOI 10.1261/rna.629607.
40. Lauhon, C. T.; Szostak, J. W. J Am Chem Soc 1995, 117, 1246–1257.
41. Travascio, P.; Bennet, A. J.; Wang, D. Y.; Sen, D. Chem Biol 1999, 6, 779–787.
42. Paul, N.; Springsteen, G.; Joyce, G. F. Chem Biol 2006, 13, 329–338.
43. Li, Y.; Liu, Y.; Breaker, R. R. Biochemistry 2000, 39, 3106–3114.
44. Wang, W.; Billen, L. P.; Li, Y. Chem Biol 2002, 9, 507–517.
45. Achenbach, J. C.; Jeffries, G. A.; McManus, S. A.; Billen, L. P.; Li, Y. Biochemistry 2005, 44, 3765–3774.
46. McManus, S. A.; Li, Y. Biochemistry 2007, 46, 2198–2204.
47. Salehi-Ashtiani, K.; Szostak, J. W. Nature 2001, 414, 82–84.
48. Chinnapen, D. J.; Sen, D. Proc Natl Acad Sci USA 2004, 101, 65–69.
49. Chinnapen, D. J.; Sen, D. J Mol Biol 2007, 365, 1326–1336.
50. Cheglakov, Z.; Weizmann, Y.; Beissenhirtz, M. K.; Willner, I. Chem Commun 2006, 3205–3207.
51. Cheglakov, Z.; Weizmann, Y.; Basnar, B.; Willner, I. Org Biomol Chem 2007, 5, 223–225.
52. Tian, Y.; He, Y.; Mao, C. ChemBioChem 2006, 7, 1862–1864.
53. Xiao, Y.; Pavlov, V.; Gill, R.; Bourenko, T.; Willner, I. ChemBioChem 2004, 5, 374–379.
54. Pavlov, V.; Xiao, Y.; Gill, R.; Dishon, A.; Kotler, M.; Willner, I. Anal Chem 2004, 76, 2152–2156.
55. Li, D.; Shlyahovsky, B.; Elbaz, J.; Willner, I. J Am Chem Soc 2007, 129, 5804–5805.
56. Liu, J.; Lu, Y. Angew Chem Int Ed 2006, 45, 90–94.
57. Hansen, J. A.; Wang, J.; Kawde, A. N.; Xiang, Y.; Gothelf, K. V.; Collins, G. J Am Chem Soc 2006, 128, 2228–2229.
58. Höbartner, C.; Pradeepkumar, P. I.; Silverman, S. K. Chem Commun 2007, 2255–2257.
59. Höbartner, C.; Silverman, S. K. Angew Chem Int Ed 2007, 46, in press. DOI 10.1002/anie.200702217.
60. Tarasow, T. M.; Tarasow, S. L.; Eaton, B. E. Nature 1997, 389, 54–57.
61. Seelig, B.; Jäschke, A. Chem Biol 1999, 6, 167–176.
62. Serganov, A.; Keiper, S.; Malinina, L.; Tereshko, V.; Skripkin, E.; Höbartner, C.; Polonskaia, A.; Phan, A. T.; Wombacher, R.; Micura, R.; Dauter, Z.; Jäschke, A.; Patel, D. J. Nat Struct Mol Biol 2005, 12, 218–224.
63. Nowakowski, J.; Shim, P. J.; Prasad, G. S.; Stout, C. D.; Joyce, G. F. Nat Struct Biol 1999, 6, 151–156.

Reviewing Editor: Gary Glick